

X-ray magnetic circular dichroism spectra and distortions at Fe²⁺ L_{2,3} edges

Xin Wang ^a, Frank de Groot ^b and Stephen P. Cramer ^a

^aDepartment of Applied Science, University of California, Davis, CA 95616

^bSolid State Physics, University of Groningen, The Netherlands

We have shown from ligand field multiplet calculations that the shape of X-ray magnetic circular dichroism (XMCD) spectra changes drastically with the distortion parameter D_s . The temperature dependence study of XMCD makes it possible to determine both D_s and spin-orbit coupling.

1. INTRODUCTION

X-ray magnetic circular dichroism (XMCD) is a new experimental technique with promising future for site-specific characterization of metals in complex. By observing the XMCD signal, we can investigate the magnetic and electronic structure of 3d transition metals and rare earth compounds. XMCD was predicted theoretically by Thole *et al.* (1) using ligand field multiplet calculations, and experimentally then demonstrated at the L₃ and L₂ edges of transition metals (2-3). XMCD spectra of transition metal ions have been calculated in O_h symmetry (4). There are several powerful sum rules being developed (5) which allow determination of the average values for $\langle S_z \rangle$ and $\langle L_z \rangle$.

In this paper, we demonstrate that the shape of XMCD spectra changes drastically not only with a crystal field, exchange field and spin-orbit interactions, but also with the presence of distortion for a certain ground state. When the distortion is in the same order of the spin-orbit interaction, the ground state character changes with the distortion parameter D_s , and some

excited states cross the ground state. In some cases the energy splitting is very small, causing the XMCD spectra shape to be very sensitive to temperature.

2. GROUND STATE CHARACTER OF TETRAGONAL DISTORTIONS

The effect of distortion on XMCD spectra is studied for high-spin Fe²⁺ L_{2,3} edges. In the ligand field multiplet calculations, the transition channels for d⁶ L edge can be approximated as 2p⁶3d⁶ → 2p⁵3d⁷. The ground state ⁵D₄ in spherical symmetry O(s) is reduced to ⁵T₂ in the presence of a crystal field with octahedral symmetry O_h. A magnetic field along the z axis lower the symmetry further to C₄ and the exchange field is included by a Zeeman term in the Hamiltonian. As shown in Fig 1, which represents the single particle picture, the 3d orbitals are split into t_{2g} and e_g levels with an energy difference of 10 Dq. When there is a weak field along the z axis and stronger field along the x and y axes, the octahedron is elongated along the z axis, and the degeneracy of t_{2g} (d_{xy}, d_{yx}, d_{xz}) and e_g (d_{z²}, d_{x²-y²}) are removed. The distortion is represented

by the ligand field parameter D_s . The T_2 , E , T_1 , A_1 , T_1 and T_2 levels which derive from the $5T_2$ configuration through spin-orbit interaction (6) will split further, and each state gives different XMCD spectra. When D_s changes sign, the elongated shape changes into a compressed one, and the energy level ordering of the xy and xz , yz orbitals reverses, therefore the ground state symmetry changes from e_g to b_2 .

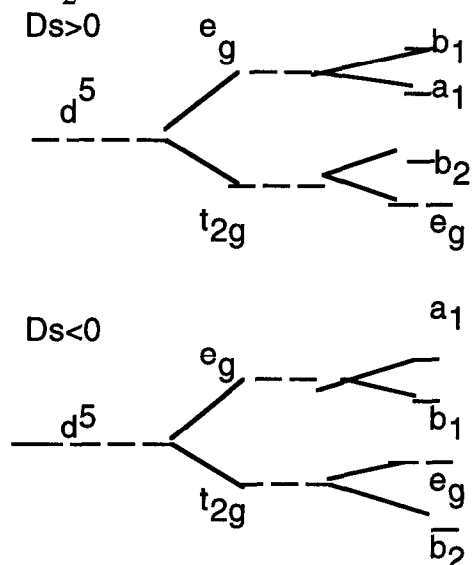


Figure 1. Ground state symmetry with the presence of tetragonal distortions.

3. RESULTS AND DISCUSSIONS

The XMCD spectra calculated with different D_s values at $T=0K$ are presented in Figure 2. All the coulomb interaction and exchange integrals are scaled to 80%. The exchange field is included by a term $g\mu_B H S$ in the Hamiltonian with $\mu_B H=0.001$ eV. The crystal fields of $10Dq=1.0$ eV and $Dt=0.0$ eV were used to simplify the analysis. The core hole lifetime was taken into account by broadening the spectra with a Lorentzian width of 0.3

eV and a Gaussian width of 0.2 eV.

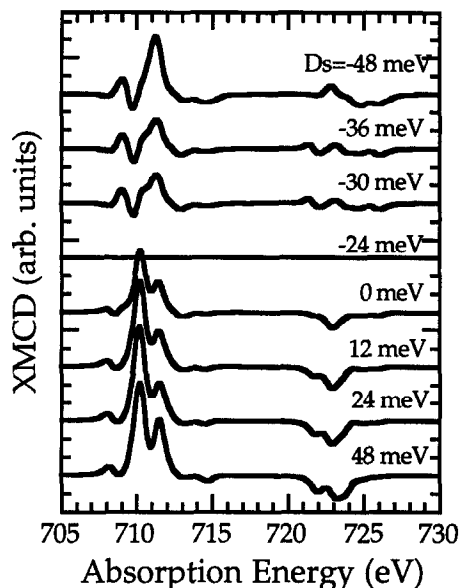


Figure 2. XMCD spectra as a function of distortion D_s .

Both the XMCD spectra shape and intensity change drastically with D_s . For $D_s=-24$ meV, there is no observable MCD effect at 0 K. With an increase of negative D_s , the L_3 edge shows a larger MCD effect around 711 eV and a well separated small peak around 709 eV. The intensity increase is almost 50% at the L_3 when changing D_s from -30 meV to -48 meV, and L_2 becomes much broader. For positive D_s , the XMCD spectra are very different. The L_3 peaks are much sharper around 710 eV, which is about 1 eV lower energy than the L_3 peak for negative D_s . There is also a shoulder on 1.5 eV higher energy side. From $D_s=0$ to 48 meV, the MCD effect at L_3 gradually increases and becomes more distinguishable at the L_2 edge.

Figure 3 presents the energy level diagram for square planar symmetry. The number shown on the top gives the

approximate expectation values of $\langle S_z \rangle$ except for $D_s=0$, where $\langle S_z \rangle = -1$ and 1 should be respectively -1.53 and 1.52 .

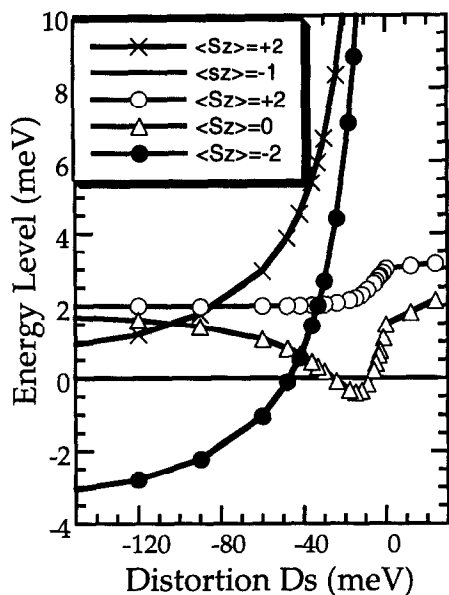


Figure 3. Five lowest energy level diagram as a function of D_s .

For positive D_s , the lowest energy level remains lowest, which is consistent with that there is no "sudden" changes in the XMCD spectra. For negative values of D_s , there are three clear transitions, one near -8 meV, one around -24 meV and the last one at -42 meV. At $D_s = -8$ meV, the $\langle S_z \rangle = 0$ line crosses the $\langle S_z \rangle = -1$ line and becomes the ground state due to the coupling of the ground states to the excited states. At $D_s = -24$ meV, the $\langle S_z \rangle = 0$ line crosses $\langle S_z \rangle = -1$ again and $\langle S_z \rangle = -1$ is the ground state. At $D_s = -42$ meV, a phase transition occurs where a 'spin-orbit' excited state with $\langle S_z \rangle = -2$ becomes the ground state. This is a similar effect as the high-spin low-spin crossings in the Tanabe-Sugano diagrams, which comparing 'Coulomb exchange' and cubic crystal field instead of 'spin-orbit' and ' D_s '.

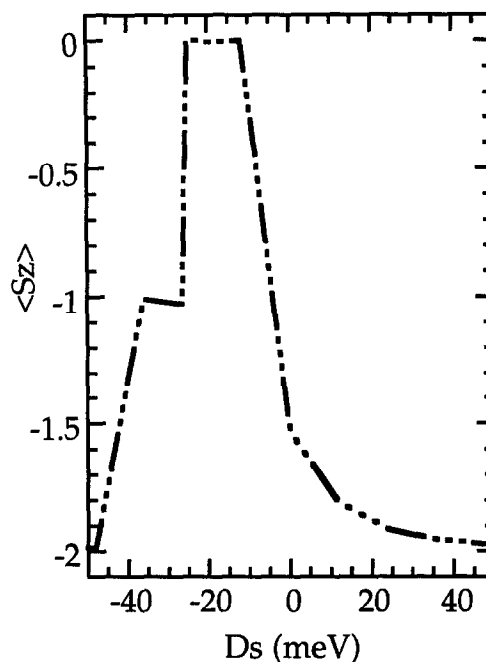


Figure 4. Ground state expectation value $\langle S_z \rangle$ as a function of D_s .

In Figure 4, we show the expectation values of the spin moment in the z direction $\langle S_z \rangle$ at the ground state. When the two lowest states cross, there is a jump in $\langle S_z \rangle$ at 0 K. The ground state $\langle S_z \rangle$ shows a strong dependence on D_s : between -8 meV and -24 meV, $\langle S_z \rangle = 0$ is the ground state, therefore no MCD effect will be observed for such a system. The strongest dichroic effect is not observed at 0 K here, as shown in Figure 5 and 6. Mixing of higher energy levels with higher $\langle S_z \rangle$ values will give larger MCD. For $D_s = -26$ meV, half of the dichroic effect of $\langle S_z \rangle = -2$ ground state is expected since $\langle S_z \rangle = -1$ is the ground state. For $D_s = -48$ meV, the ground state is almost $\langle S_z \rangle = -2$. Increase of positive D_s values gradually shift the ground state into a pure $\langle S_z \rangle = -2$ state.

Figure 5 and 6 illustrate the

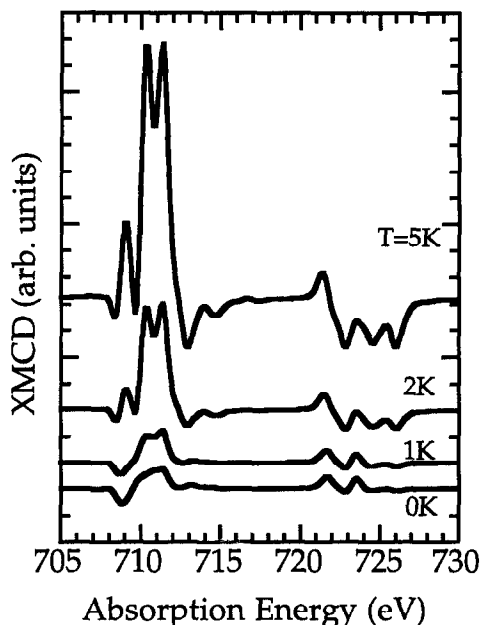


Figure 5. Temperature dependence of XMCD spectra at $D_s = -12$ meV.

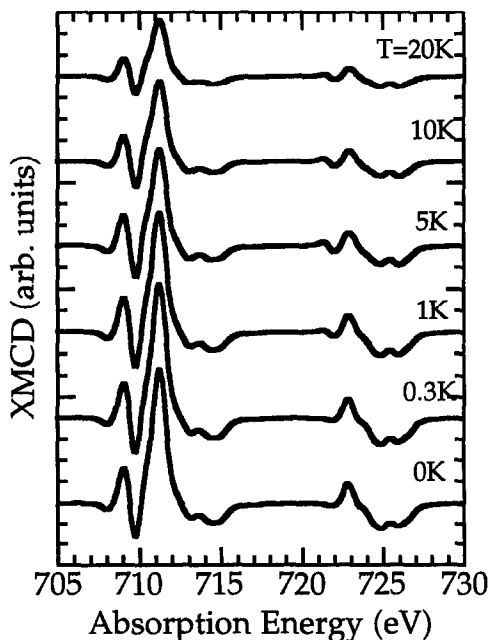


Figure 6. Temperature dependence of XMCD spectra at $D_s = -48$ meV.

temperature dependence of the XMCD

spectra for a given value of D_s . For $D_s = -12$ meV, as shown in Figure 5, there is almost no dichroic effect at 0K, but with an increase of temperature to 5K, a weak MCD spectrum is expected. When $D_s = -48$ meV, higher temperature reduces the MCD, as the higher levels are with lower $\langle S_z \rangle$ values. The temperature dependent XMCD study makes it possible to determine both spin-orbit coupling and D_s values.

4. CONCLUSIONS:

From ligand field multiplet calculations, we have shown that for the high-spin d^6 , the XMCD spectra shape changes drastically with the presence of distortions. The character of the ground state changes when D_s changes sign, and mixings of different states could yield no dichroic effect at 0K for certain distortions. XMCD spectra also show a strong temperature dependence which allows determination of both spin-orbit coupling and D_s values. This calculation can be generalized to all 3d transition metals.

REFERENCES

1. B. T. Thole, G. van der Laan, G. A. Sawatzky, *Phys. Rev.Lett.*, 55 (1985), 2086.
2. C. T. Chen, F. Sette, Y. Ma, S. Modesti, *Phys. Rev. B*, 42 (1990), 7262.
3. C. T. Chen, N. V. Smith, F. Sette, *Phys. Rev. B*, 43, (1991), 6785.
4. G. van der Laan, B. T. Thole, *Phys. Rev. B.*, 43 (1991), 13401.
5. B. T. Thole, P. Carra, F. Sette, G. van der laan, *Phys. Rev. Lett.* 68 (1992), 1943.
6. F.M.F. deGroot, *J. Elec. Spec.* 67, (1994), 529.